Membrane Technology
ISSN (online): 1873-4049

Research on the Comprehensive Test Method for the Characteristics of Generator De-Excitation Switch

Jingguang Yang[1], Shaoxin Liu[1], Jiazhi Zhang[1], Jinsong Gao[1], Xiaoyong Lv[1], Ju Zhao[1], Zhenhong Gong[2, *], Huan Guo[2]

[1]*China Yangtze Power Co., Ltd., Yichang 443000, Hubei, China*
[2]*Jinan University, Zhuhai, 519070, Guangdong,China*
**Corresponding Author.*

Abstract:
This paper proposes a comprehensive test method to meet the multi-functional testing requirements of de-excitation switch, which can simplify the complex test process and greatly reduce the cost of testing. A comprehensive test topology was designed based on the requirements of multiple test projects, and the key parameters were intended. The test circuit generates a constant test current based on the supercapacitor, Through the shunt and the precision recording module, the method realizes the synchronous recording of the test current and the test voltage, and can accurately record the action state and action time of each break of the degaussing switch, so as to realize the switching action and synchronization performance test of the de-excitation switch. A multi-functional comprehensive test circuit simulation model was built for verification, which showed the feasibility of the circuit design. A multi-functional comprehensive test device was built for experiments, and the experimental results show that the comprehensive test device can accurately test the contact resistance of the break, accurately test the action time of the switch, and test the synchronous performance of the break, which can be used efficiently and flexibly in the on-site maintenance work.

Keywords: de-excitation switch, comprehensive test methods, supercapacitor, contact resistance, switch action, synchronous recording wave.

INTRODUCTION

When the fault occurs, the de-excitation switch will quickly isolate the generator winding from the inspiration circuit. Therefore, the reliability of the de-excitation switch is critical to the safe of the generator and the stable operation of the power system. The maintenance and testing of the de-excitation switch are required regularly[1].

The de-excitation switch characteristic test mainly includes the test of the contact resistance of the break, the switching action test, and the synchronization performance test[2-4]. For the test of the contact resistance of the break, Liu et al. and Zhang et al.[5,6] proposed through experiments that the voltage source provides a 0-100A adjustable current, which improves the accuracy of measuring on-state resistance by changing the measurement point of the contact resistance. Xia et al.[7] based on a method of producing a kiloampere-level impulse current with capacitors, realizes a resistance detection loop with a peak current of 1,000A.

For the study of the switching action test, the key of multi-channel wave recording is the accurate measurement of multi-state points in the recording system when the instruction is decentralized[8]. Hu et al.[9] designed a high-voltage circuit breaker test system that can synchronously sample the contact state in 4 channels, in which the sample rate reaches 29kHz, and the multi-channel recording wave interval is less than 4ns. Du et al.[10] designs an operation platform based on the test of isolation switch action with an attitude sensor, which reduces the detection cost while ensuring detection accuracy.

For the synchronous performance test, Li and Jiao[11] uses DSPVC33 as the main controller and uses a distributed circuit breaker detect device as the core to detect information such as the time itinerary of the circuit breaker switching process. The experiment shows that the delay is shorter than that in the conventional detection method.

In summary, the testing current is often 250A, while the 1000A impulse current test makes it difficult to reflect the situation of the de-excitation switch in a long-running time[12]. The recording wave channel in some de-excitation switch tests requires more than 7, while the recording wave channel of the instrument is often not enough to detect all the breaks of the de-excitation switch at the same time[13]. In addition, the de-excitation switch test is mainly for a single experiment content, and there is still a lack of research and development for the comprehensive test of the de-excitation switch.

To solve the problems above, this paper proposes a comprehensive test method of the de-excitation switch characteristic, which is functional and accurate. This method is capable of performing a variety of tests such as the resistance test at microohm level and the switching action test, which improves the convenience and efficiency of the test.

TEST PRINCIPLES AND TEST REQUIREMENTS

Test Principles

This paper takes the CEX series of de-excitation switches as an example. The comprehensive test circuit design is shown in Figure 1.

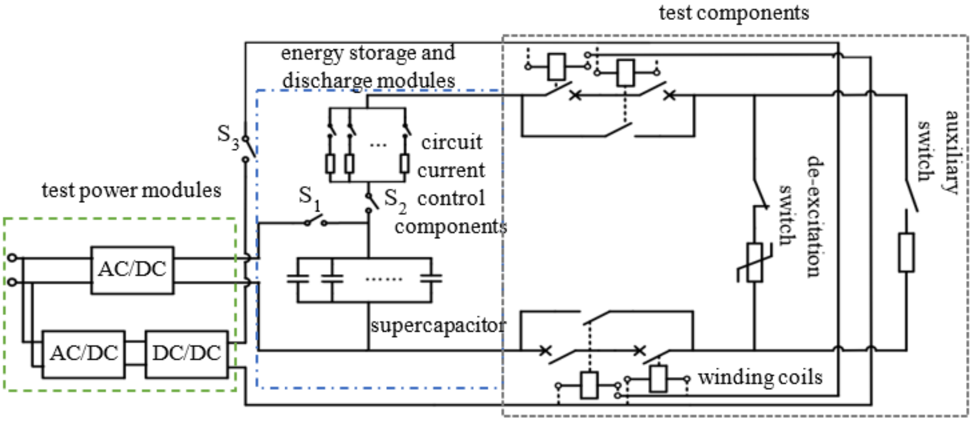

Figure 1. Comprehensive test circuit topology

The device circuit is divided into test power modules, energy storage and discharge modules, and test components. The test power module contains a separate AC/DC module to provide 12V voltage to charge the supercapacitor. In addition, AC/DC and DC/DC modules offer adjustable coil operating voltages ranging from 60V to 250V. Energy storage and discharge modules include supercapacitors and circuit current control components, which control the current in the load component by adjusting the status of the relay, and provide the test constant current with the supercapacitors. The test components include winding coils, the de-excitation switch, control relays, and the auxiliary switch. The auxiliary switch consists of a controllable relay and resistor in series. On the test platform, the machine controls the status of relay S1-S3 to meet the test circuit reconstruction of different experiments, as shown in Table 1.

Table 1. On-off state

function	S_1	S_2	S_3
supercapacitors charging	1	0	0
the test of the contact resistance of the break	0	1	1
the switching action test	0	1	1

The main break and the arc breaks in the de-excitation switch are connected in parallel. When the two breaks are turned on at the same time, the current of the separate branch cannot be determined. Therefore, the contact resistance test is divided into pre-test and formal test. In the experiment, the supercapacitors and circuit current loads output the constant test current of 1500A for 10s by closed-loop control. After the voltage drop of the contact resistance is estimated, the main break is closed and the test is performed again.

Take the closing test of the switching action test as an example. Before the experiment, the main break and the arc breaks are opened, and the discharge break is closed[14]. During the experiment, the energy storage discharge module outputs the 300A test current and then drives the closing coil in different voltages to detect the operating characteristics of the de-excitation switch. The operation of the refusal test and opening test is similar to that of the closing test.

During the synchronization performance test, the time of each action of the de-excitation switch is recorded, which includes the time when the switch began to move and the time when the break actually opened or closed. Collect the voltage signal through the recording wave and draw the time sequence diagram, then evaluate the synchronization performance of the de-excitation switch under different operating conditions.

Test Power Requirements

The key to the test of the contact resistance is the general state resistance in the stable working state of the switch. Its resistance value is only tens of microohms (<50μΩ)[15], and the conventional 200A test current generates a voltage drop which is only several microvolts. External noise and measurement errors have a bad impact on the measurement accuracy. The test is intended to provide a 1500A testing current by the supercapacitor[16]. After the switch runs for 10 seconds, it can reach thermal stability. At this time, the measured contact value of the test can reflect the normal working state. The power supply can be calculated based on the maximum 50μΩ resistance value, which is 112.5W, and the test power is 562.5W.

In the switching action test, under the arc voltage standard of the generator set, the closing action voltage is 80%UN, the opening action voltage is 65%UN, and the refusal voltage is 30%UN. The rated operating voltage UN is 220V[17]. The operating voltage needs to be added to both ends of the switch coil. The resistance value of the opening coil is 170.9Ω ~ 171.6Ω, and the resistance value of the closing coil is 11.0Ω ~ 11.5Ω. Set the output of the energy storage discharge module 300A, which is the test current in the circuit. The power supply is 358.39W, the power needed in the closing test is 8800W, the power needed in the rejection test is 792W, and the maximum power required for the test is 21W.

The synchronization performance test records the action time of each break based on the switch action test and analyzes it to form the time sequencing diagram. The action test focuses on whether the switch action is correct, and the synchronization test focuses on the consistency of the movement of each break during the action process[18,19]. In addition, the supercapacitors need to be charged before the test. The charging voltage is 9.6V, and the charging time is 13.6 min. The charging power is 860.16W, calculated based on the classic charging curve of the supercapacitor[20]. The requirements and technical indicators of each test are shown in Table 2. After considering a certain margin, the demand for low-voltage DC power is about 1kW, and the demand for high-voltage DC power is about 10kW. The capacitor charging power is provided by the low-voltage AC/DC module, and others are provided by the high-voltage AC/DC module.

Table 2. Multifunctional test requirement

Low voltage DC power supply requirements				
function	voltage /V		current /A	power /W
supercapacitors charging	9.6		1	860.2
High voltage DC power supply requirements				
function	voltage/V	current/A	test power /W	supply power/W
the test of the contact resistance	0.075	1500	562.5	112.5
close test	143	300	21	358.4
open test	176	300	21	8800
rejection test	66	300	21	792

TEST CIRCUIT DESIGN ANALYSIS

Energy Storage Discharge Circuit

The discharge equivalent circuit of the supercapacitor bank is shown in Figure 2.

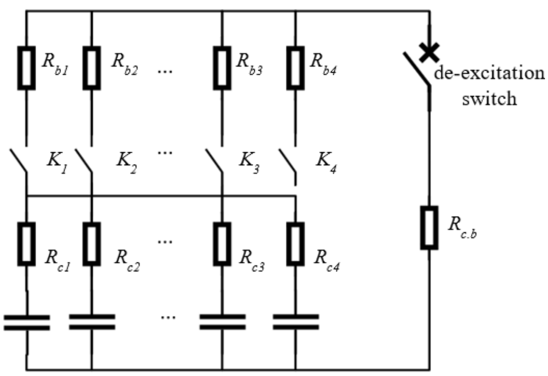

Figure 2. Supercapacitor bank discharge equivalent circuit

where C_1~C_n are the parallel capacitances in the supercapacitor bank, R_{b1}~R_{bn} are the load resistors of the regulation loop, R_{c1}~R_{cn} are the equivalent internal resistors of the supercapacitors, and K_1~K_n are current relays that control resistors access. $R_{c.b}$ is the equivalent contact resistor of the de-excitation switch.

Assume that the total capacitance value of the supercapacitor bank is C and its voltage is u_C, the resistance value of the load component controlled by the loop current at a certain time is r(t). The analytical expression of the test loop is shown in (1). The resistance of the object itself is much smaller than the resistance of the loop current control load component, so it can be omitted in the analytical model.

$$r(t)C\frac{du_{\mathrm{C}}(t)}{dt}+u_{\mathrm{C}}(t)=0 \quad (1)$$

The charging voltage of the supercapacitor is set to U_0, and the initial value of the test loop current $i(t_0)=0$. The current during the test is shown in (2).

$$i(t)=\frac{\mathrm{U}_0}{r(t)}e^{-\frac{t}{r(t)\mathrm{C}}} \quad (2)$$

In the actual test, the ideal state of the current should be maintained at constant, which means $i(t)=I_N$. The analytical expression of the load component resistance is shown in (3). The current can be controlled by controlling the relays in the load component according to this equation.

$$r(t)=-\frac{t}{C*\mathrm{ProductLog}\left[-\frac{\mathrm{I_N}t}{C\mathrm{U}_0}\right]} \quad (3)$$

According to the requirements of the de-excitation switch contact resistance test, the supercapacitor bank provides a constant current of 1500A for at least 10 seconds, which is designed according to 1500A/10S (15KAS), and the specification of a single capacitor is selected as 3V(3.2V)/3400F. The estimated resistance of the test circuit is about 5.9mΩ, and the capacitor voltage needs to be at least 8.8V. When the discharge capacity reaches the desired level, the capacitor voltage drops to about 0.8V. Considering the capacitor specification, its initial voltage is appropriate to be 9.6V. The component placement is specified on every 3 capacitors in series and 28 series are connected in parallel, a total of 84 capacitors are composed. The supercapacitors are distributed in two capacitor packs and placed in the same chassis.

The loop control load-weighted resistance network is shown in Figure 3, where R_1~R_n are power resistors and K_1~K_n are relay switches. The relay switch is flexibly turned on and off according to the capacitor voltage, thereby achieving real-time adjustment of the load resistance and obtaining flexible control of the test current.

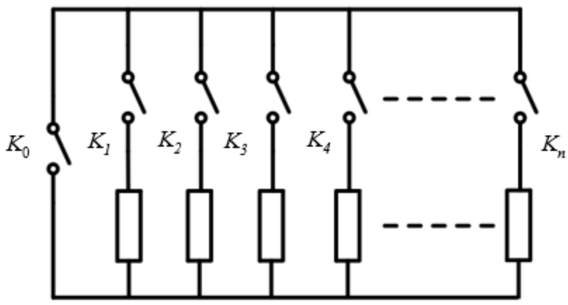

Figure 3. Loop control load resistance network

The power resistance of each branch in the network has the following relationship: $R_1=2R_2$; $R_2=2R_3$; $R_3=2R_4$; ……; $R_{n-1}=2R_n$. When only K_1 is closed, the total resistance of the network is the largest, which is $R_{max}=R_1$. When all switches are closed, the total resistance of the network is the smallest, $R_{min}=0.5R_n$. From (3), it can be obtained that the minimum resistance R_{min} of the network needs to be less than 6.4mΩ, and the maximum resistance R_{max} of the network needs to be greater than 60mΩ. Therefore, R_1=100mΩ; R_n=5.9mΩ.

Contact Resistance Test Circuit Design and Analysis

The equivalent circuit of the contact resistance test is shown in Figure 4. In order not to affect the control current of the resistive load component, the resistor R connected in series with the auxiliary switch is selected to be 0.1 mΩ.

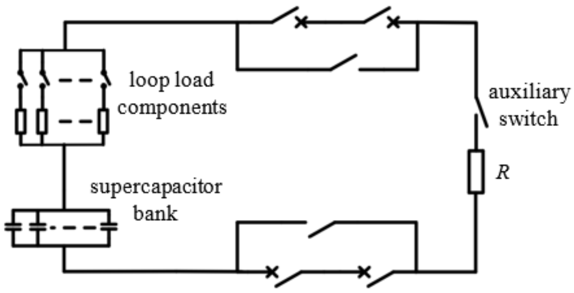

Figure 4. Contact resistance test equivalent circuit

The on-state resistance measurement accuracy must reach the microohm level. When using a shunt to measure resistance, the loop current flows directly through the shunt to generate a voltage drop, which is not easy to produce interference[21,22]. The shunt specification selected for this test is 2000A/75mV, and the measurement accuracy is 1‰-3‰. The signal pickup of the shunt adopts the high-impedance acquisition mode, as shown in Figure 5. The filter amplifier circuit has the characteristics of high input impedance and high common-mode rejection ratio, and its measurement accuracy reaches 0.3‰-0.5‰. The total accuracy of the measured waveform can be obtained as (4).

$$\sigma_{total} = \sqrt{\sigma_1^2 + \sigma_2^2} \tag{4}$$

σ_1 is the measurement accuracy of the shunt, σ_2 is the measurement accuracy of the filter amplifier circuit, and the total accuracy of the current measurement and recording is calculated to be approximately 3.2‰-5.8‰.

The voltage drop signal of the circuit breaker is collected and input into the filter amplifier circuit with the same structure as above. After correction, it enters the recording system to complete the voltage measurement of the circuit breaker with an accuracy of 0.3‰-1‰±0.1mV.

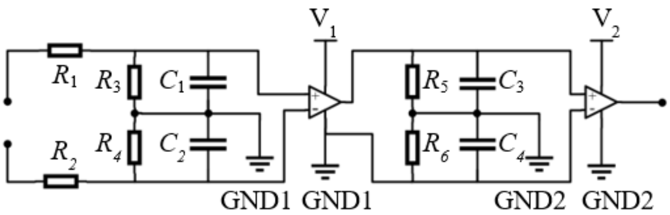

Figure 5. Filter amplifier circuit

According to the above parameters, a simulation model was built in Simulink for verification. The output current was set to 1500A. The circuit load impedance and current change waveforms are shown in Figure 6. The control step size is 0.1s.

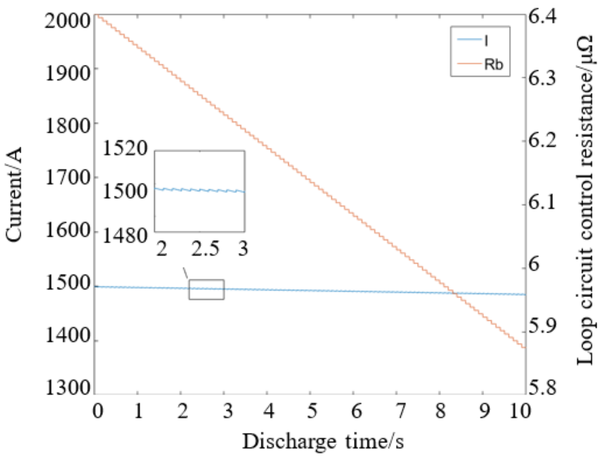

Figure 6. Circuit load impedance and current change waveform

An equivalent simulation model was built in Simulink software for verification. The contact resistance of the four arc break ports was estimated during the pre-test, and then the main switch was connected back and closed to formally test the main break port. The results are shown in Figure 7, taking the voltage and current waveforms of arc break port 1 as an example.

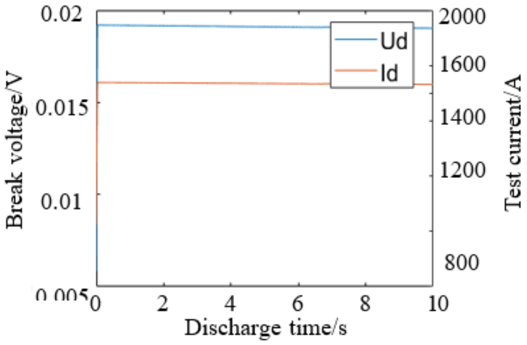

Figure 7. Arc break contact resistance

Experiments are completed based on the above setup. The testing current and test time are set at 30kA and 15 seconds, respectively. Before the experiment starts, the supercapacitor bank is charged to 12V. The charging circuit is then disconnected to start the experiment. The contact resistance is calculated from the voltage and current obtained at the break. The contact resistance of arc break 1 is 13μΩ.

Design and Analysis of Switch Synchronization and Synchronization Performance Test Circuit

The equivalent circuit of the switching action test and synchronization performance test is shown in Figure 8. In the circuit, the supercapacitor produces a 300A test current for the loop, and the action time is less than 500ms. From **Error! Reference source not found.**, it is derived that when t = 1s, the loop current decreases to 299.45A. Consequently, the loop current can be directly provided by the supercapacitor in series with the initial load resistance.

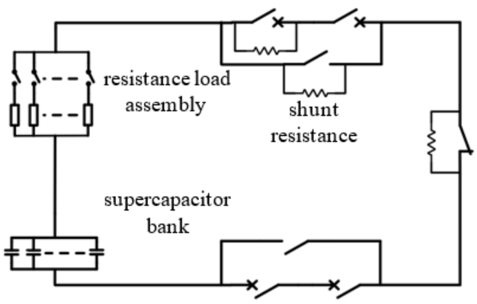

Figure 8. Switching action and synchronization performance test equivalent circuits

During the action test, each break is paralleled by a shunt resistor. While ensuring that the current source provided by the capacitor is never open-circuited, the wave recording system captures the voltage drop signals of the shunt resistor. The moment of voltage jump is the moment of the break action [23]. The resistance value of this shunt resistor can be selected as 0.1mΩ.

Each break requires an individual wave recording board for measurement, sharing a 485 bus, and the time difference between the seven recording boards should not exceed 8ms. The signals filtered are converted from analog to digital and stored in RAM through an A-D conversion. The command coordination is controlled by the CPU, which receives instructions from the upper computer and transmits the A-D converted data through a filter amplification circuit to the computer. Figure 9 illustrates the schematic diagram of the recording circuit.

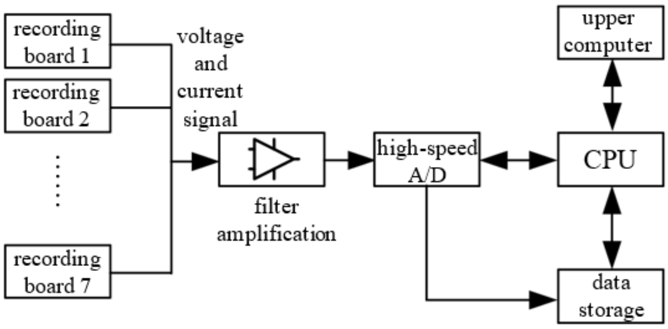

Figure 9. Structure diagram of the wave recording module

An equivalent simulation model is built in Simulink software for verification. During the closing test, the voltage waveforms of each break are shown in Figure 10. The simulation time is set to 1s, and the voltage jump time is the break action moment.

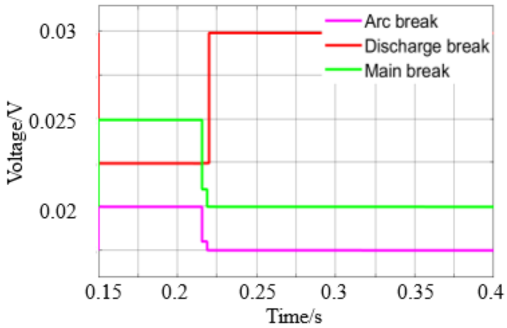

Figure 10. Voltage drop at each break during closing

The main break and arc breaks are in parallel, and the two arc breaks are connected in series. The voltage of the main break is constantly twice that of the arc break. After 0.262s, the arc break closes, and the equivalent resistance decreases, thus the voltage drop reduces. Consequently, the voltage of the main break also decreases due to the parallel relationship. Similarly, after 0.275 s, the main break closes, and the voltage drop reduces, which also leads to a decrease in the voltage drop of the arc break. After 0.28s, the discharge interrupter opens, since it is in series with the other two breaks, the on-state resistance of the circuit increases, which causes a slight decrease in the voltage of the main break and arc breaks, and a drop in the voltage of the discharge break.

During the opening test, the voltage waveforms of each break are shown in Figure 11. The main break opens first, increasing the voltage drop. Subsequently, the arc break closes, reducing the voltage drop, which is equivalent to a decrease in the circuit resistance, causing the voltage drop of the main break and arc breaks to rise. Finally, the arc break opens, increasing the voltage drop.

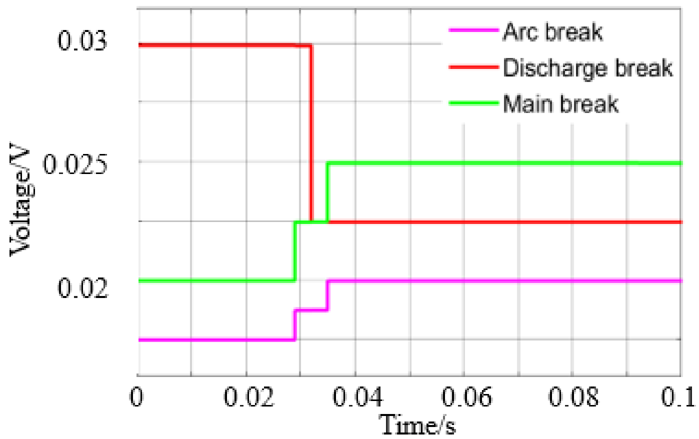

Figure 11. Voltage drop at each break during opening

PLATFORM CONSTRUCTION AND EXPERIMENTS

Platform Building

To validate the reliability and efficiency of the comprehensive test method proposed in this paper, a multifunctional testing device for de-excitation switches based on the comprehensive test method has been developed, as shown in Figure 12. The equipment in the figure is the test platform.

Figure 12. De-excitation switch multi-function test device physical diagram

Switch Simulation Test

The equipment is used to measure the resistance value of a switching device, and the measurement results are shown in Figure 13. in the form of the curve of loop current and the voltage drop of the switch. The test results indicate that within the range of 9ms to 60ms, the switch resistance voltage drop is 1031mV, and the main circuit loop current is 1500A. The ratio of these two values is the dynamic resistance of the switch, which is 688μΩ. During the measurement process, the current ripple is minimal, and the switch resistance curve is stable, indicating a good measurement outcome.

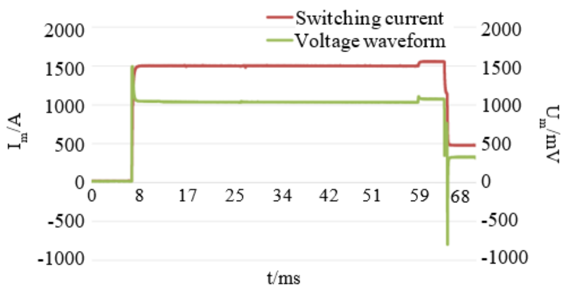

a) Switching current and voltage waveform

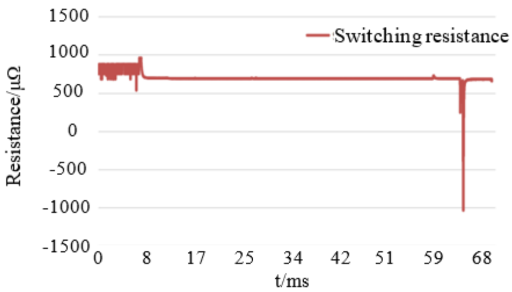

b) Switching resistance waveform

Figure 13. Test result of contact resistance measurement of de-excitation switch

Synchronous Performance Testing and Action Testing

In the synchronization performance test, the chronological sequence of action for each break is shown in Figure 14. During the closing process, the action time of main break 1 and main break 2 is 274ms and 275ms respectively, and the four arc breaks operate between 261ms and 263ms, and the discharge auxiliary break operates at 280ms. The closing time is 280ms in total. During the opening process, both main break 1 and main break 2 operate at 29ms, the four arc breaks operate at 35ms, and the discharge auxiliary break operates at 35ms. The opening time is 35ms in total. The test results indicate that the de-excitation switch has good synchronization performance. The timing sequence is compliant and the synchronization performance of the de-excitation switch meets the standards.

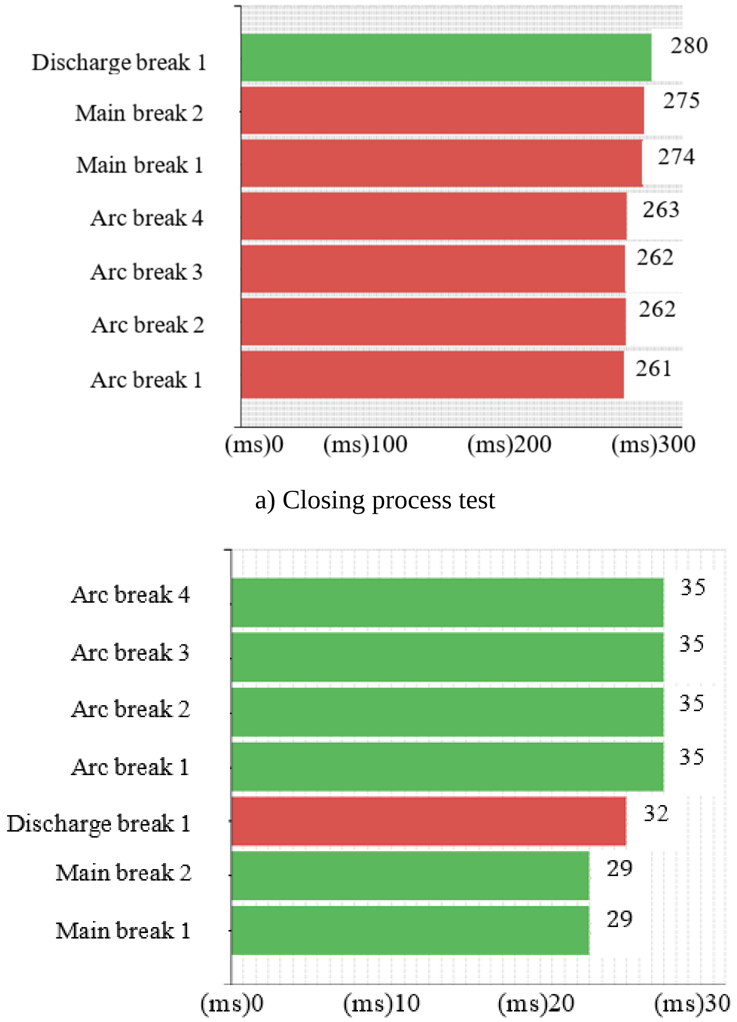

a) Closing process test

b) Opening process test

Figure 14. Test result of synchronization performance of de-excitation switch

Five action tests are performed by applying different voltage levels to the coil, and the results are presented in Table 3. The average closing time is 280ms, and the average opening time is 35ms. The switch has a good rejecting performance at 66V. All results are satisfactory and the operational performance meets the standard.

Table 3. Test results of switch opening and closing

Test item	Test result
176V close test	All tests showed favorable
143V open test	All tests showed favorable
66V rejection test	Good
Closing time	280ms
Opening time	35ms

CONCLUSION

The reliability of de-excitation switch is crucial for the safety of the generator itself and the stable operation of the power system. This paper takes the CEX series de-excitation switches from French company LENOIR as the test subject and proposes a comprehensive testing method that can meet the requirements of multifunctional testing. A comprehensive test topology is designed based on the needs of multiple test items, and key parameters are designed. A constant test current is generated with the supercapacitor, and the test current and test voltage are synchronously recorded through a shunt and a wave recording module, which allows for the accurate recording of the action status and action time of each break of the de-excitation switch, achieving the test of switching action and synchronization performance of the de-excitation switch. A multifunctional integrated test device is built for characteristic testing experiments, precisely measuring the contact resistance, accurately recording the action time of each break, and conducting synchronization performance test. The multifunctional test device simplifies the test process and greatly reduces the cost of the test.

ACKNOWLEDGEMENT

The work is supported by the China Yangtze Power Co., Ltd. technology project (Project No. Z222302022) .The authors express their profound gratitude to Mr. Shusheng Lin and Mr. Weiming Li from eTocsin Inc. for their invaluable support in the research endeavor and for supplying the crucial experimental data.

REFERENCES

[1] X. Sun, Y. Bao, L. Wang, J. Zhang, B. Hang, “An arcless deexcition device for hydro-generators,” Electric Engineering, no. 5, pp. 221-223, Mar. 2024.

[2] J. Dong, B. Dou, T. Yu, Q. Li, J. Yu, C. Chen, “Analysis and Solution of the De-exitation Breaker Abnormal,” Hydropower and Pumped Storage, vol. 8, no. 2, pp. 113-116, Apr. 2022.

[3] L. Gao, L. Xiao, “Analysis and Recommendation on Contact Overheat of Low-voltage Field Discharge Switch,” Jiangsu Electrical Eagineering, vol. 33, no. 1, pp. 54-55, Jan. 2014.

[4] S. Feng, R. Hu, X. Zhou, “Maintenance and practice of DC field switch for excitation system,” Mechanical & Electrical Technique of Hydropower Station, vol. 43, no. 8, pp. 28-29, Aug. 2020.

[5] X. Liu, L. Yang, A. Li, “Circuit Resistance Test Analysis of Gas Insulated Metal-enclosed Switchgear,” Shanxi Electric Power, no. 2, pp. 15-18, Apr. 2024.

[6] Y. Zhang, J. Chen, X. Qin, Y. Gu, “An expanded loop wiring method in DC resistance and loop resistance measurement,” Electrical Engineering, vol. 21, no. 12, pp. 110-112, Dec. 2020.

[7] X. Xia, R. Chen, B. Zhang, L. Zhou, T. Lu, “Study on testing circuit breaker loop resistance with high impulse current method,” Electrotechnics Electric, no. 7, pp. 37-41, Jul. 2013

[8] S. Xiao, Y. Deng, S. Lin, “Development of performance test system of super large circuit breaker based on precision wave recording technology,” Electrotechnical Application, vol. 37, no. 14, pp. 77-80, Jul. 2018.

[9] Y. Hu, H. Cheng, F. Zhang, Q. Liu, “Dynamic resistance tester for high voltage circuit breaker,” High Voltage Engineering, no. 1, pp. 105-106, Jan. 2006.

[10] F. Du, G. Wang, H. Zhang, Y. Gong, D. Ge, “A detection platform of attitude sensor system used for double reconfirmation technology of disconnecting switch's opening and closing position,” Electric Power, vol. 52, no. 11, pp. 153-158. Nov. 2019.

[11] J. Li, S. Jiao, “High voltage circuit breaker state online detection device based on DSP,” Electric Power Automation Equipment, no. 8, pp. 44-47, Aug. 2004.

[12] G. Liu, W. Li, D. Jiang, “Study on measurement of the contact resistance of electric apparatus,” Electrical Measurement & Instrumentation, no. 2, pp. 15-16, Feb. 2001.

[13] X. Chen, X. Hu, X. Shao, B. Zhu, “Evaluating on large extinguish excitation switcher agency abroad,” Large Electric Machine and Hydraulic Turbine, no. 4, pp. 69-71, Aug. 2004

[14] L. Zhao, X. Wu, Z. Wang, M. Zhao, X. Huang, "Simulation research on circuit breaker operating mechanism based on coil current," Electrical Measurement & Instrumentation, vol. 57, no. 12, pp. 9-13, Jun. 2020.

[15] Z. Yin, "Study on the influence of contact resistance on contacts of low voltage electrical equipment," Electrical Equipment and Economy, no. 5, pp. 16-18, May. 2024.

[16] K. Wu, T. Yang, "Analysis and verification on the de-excitation circuit′s parameters and performance with de-excitation simulation," Zhejiang Electric Power, vol. 29, no. 5, pp. 1-5, May. 2010.

[17] M. Liu, "Application of CEX98 series de-excitation switch in hydropower plant," in Proceedings of the 2009 Annual Meeting and Academic Exchange of Power System Automation Special Committee of China Hydropower Engineering Society, Yunnan, China, Sep. 2009, pp. 59-63.

[18] X. Xue, W. Wang, X, Chen, "Analysis on safety of field circuit breaker of large hydropower station," Yangtze River, vol. 42, no. 17, pp. 80-83, Sep. 2011.

[19] X. Zhang, K. Zhu, "Research on 40.5 kV fast vacuum circuit breaker based on electrode-excitation drive," Electrical Measurement & Instrumentation, vol. 60, no. 5, pp. 79-84, May. 2023.

[20] H. Huang, X. Fei, G. Yang, Z. Mai, "Charging Trajectory Optimization Strategy of Supercapacitor Based on Internal Resistance Compensation," High Voltage Engineering, vol. 49, no. 4, pp. 1567-1573, Apr. 2023.

[21] L. Hou, Z. Cheng, Y. Cai, N. Pang, Y. Wang, X. Yang, "Design of tripping result detection device for release of low voltage DC circuit breaker," Electrical Measurement & Instrumentation, vol. 60, no. 4, pp. 155-159, Apr. 2023.

[22] W. Yang, P. Zhang, B. Zhang, "Numerical simulation analysis and application of breaking performance of high altitude miniature circuit breaker," Electrical Measurement & Instrumentation, vol. 59, no. 6, pp. 181-187, Jun. 2022.

[23] H. Chen, S. Yang, L. Chen, H. Zhen, S. Chen, M. Zhang, "Research on current transformer error testing technology based on field signal simulation technology," Electrical Measurement & Instrumentation, vol. 58, no. 2, pp. 133-138, Feb. 2021.